

Dielectric relaxation of pure TGS crystals

C. MÎNDRU, C. P. GANEA^a, H. V. ALEXANDRU*

Faculty of Physics, University of Bucharest, Romania

^aNational Institute of Materials Physics, Bucharest-Magurele, Romania

Pure triglycine sulphate crystals (TGS) show peculiar dielectric behavior in the ferroelectric phase, after crossing down the Curie point. Dielectric dispersion was investigated on the frequency range 1 Hz ÷ 10 MHz. Temperature was changed at a sliding rate of 0.6 °C/minute, crossing up and down, several times, the Curie point between 65 °C and -120 °C. The second component of permittivity, drawn versus the frequency, shows two types of relaxation in the ferroelectric phase, with the characteristic time of $\tau_L \sim 10^{-3}$ sec and $\tau_H \sim 10^{-7}$ seconds. The first is recognized to be related with ferroelectric domain wall relaxation (domain cropping), although not clearly understood yet. The second one is ascribed to the “critical slowing down” effect, similar to the relaxation in the paraelectric phase, above T_C . A third, middle relaxation time, seems to be a sort of interaction of the two previously mentioned relaxation mechanisms. Papers from the literature, analyzing molecular dynamics and structural changes, could not correlate the flipping time $\sim 10^{-11}$ sec of the NH_3 group of the glycine GI in the structure (the main responsible of the ferroelectric transition), with the mentioned relaxation times. Several aspects of the dielectric parameters evolution, related to the two relaxation processes on the large temperature range shall be analyzed and discussed.

(Received February 8, 2012; accepted February 20, 2012)

Keywords: Ferroelectric crystals; Triglycine sulphate; Dielectric spectroscopy; Permittivity relaxation

1. Introduction

Ferroelectric materials have been extensively studied in the last decades. Important applications have been found in electronic device applications, as pyroelectric detectors [1], candidates for nonvolatile memories, ferroelectric data storage devices and nanofabrication, in the last time. These applications need fundamental studies of domain dynamics and structure and special studies of polarization switching phenomena, even at the nanoscale [2]. Several studies were focused on relaxation phenomena of ferroelectric domain wall [3-5], lattice dynamics [6-8] and dielectric relaxation [9-11].

Triglycine sulphate crystals (TGS for short), is one of the most extensively studied ferroelectric material, particularly in order to understand the lattice dynamic changes during the second order ferroelectric transition. Hoshino et al [12] have reported the essential ferroelectric parameters of TGS crystal and the single crystal structure [13]. We have previously presented [14-20] the growth and several properties of pure and doped TGS crystals. Keve et al [21, 22] have studied structural inhibition of ferroelectric switching and dopage. Cole-Cole [23] analysis around the Curie Point (CP) and at lower temperatures was performed by Zhang [4, 5]

The ferroelectric transition was associated with the asymmetrical arrangement of the Glycine group GI versus the mirror planes m , at $y = 1/4$ and $3/4$ in the cell and the proton switch along the H-bridge between glycine groups

GII and GIII, associated with the exchange role of zwitterion between these two glycine groups [13].

In this paper the TGS crystal relaxation was investigated, while mainly studding the temperature and the frequency dependence of the imaginary component of permittivity. The higher frequency relaxation mechanism ($\tau_H \sim 10^{-7}$ seconds) was found to be practically independent from temperature. The lower frequency relaxation mechanism ($\tau_L \sim 10^{-3}$ sec), related to the ferroelectric domains evolution, has an important thermal evolution, with an activation energy of 0.7 eV (approximately 28 $k_B T$).

2. Experimental

Pure Triglycine sulphate crystals were grown in a thermostated oven at 54 °C, (i.e. in the paraelectric phase), by slow solvent evaporation. Plates of ~1 mm thick and ~0.5 cm^2 surface were cleaved perpendicular on the ferroelectric axis b and then polished and silver paste painted as electrodes.

Measurements were accomplished with Alpha-A High Performance dielectric spectrometer, Novocontrol and the Sample Cell ZGS, on the frequency range 1 Hz - 10 MHz. Five frequency values, equidistant in log scale have been chosen on every decade, i.e. 36 frequencies on the whole frequency range.

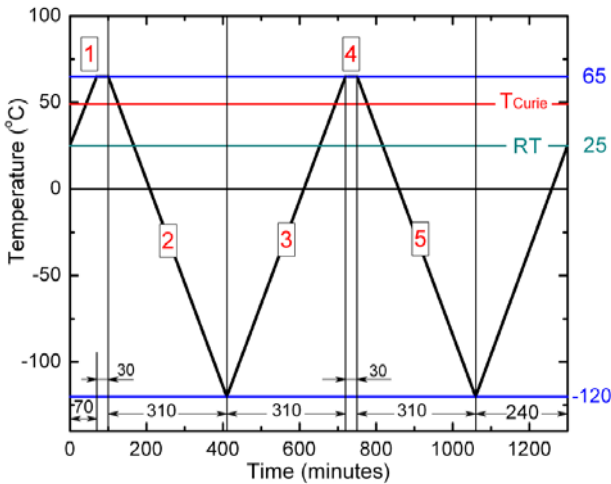


Fig. 1. The time-temperature variation during dielectric measurements.

Temperature of the sample was changed at a rate of 0.6°C/minute from room temperature to 65°C and down to -120°C, crossing up and down the Curie point several

times. The temperature evolution during measurements is presented in Fig.1.

Measurements have been performed in five successive temporal stages. In the stage {1} the room temperature of the virgin crystal was increased, crossed up the Curie point and remained constant at 65°C for 30 minutes. Thus, it was intended to “wipe off” the space charge eventually accumulated in the sample during the phase transition.

In the stage {2}, typical permittivity relaxations take place in the ferroelectric phase after crossing down the Curie point. Essential changes can be noticed in the stage {2} versus stage {1} in fig.2, for both components of permittivity. In the stage {3} important relaxation phenomena took already place compared to stage {2}, particularly in the temperature range between the room temperature and the Curie point (Fig. 2).

Stage {5} repeats quite closely the experimental data of the stage {2}, for both components of permittivity. This happens because the same pace of temperature variation has been used and the relaxation was repeated almost identically in the stage {5} versus stage {2}.

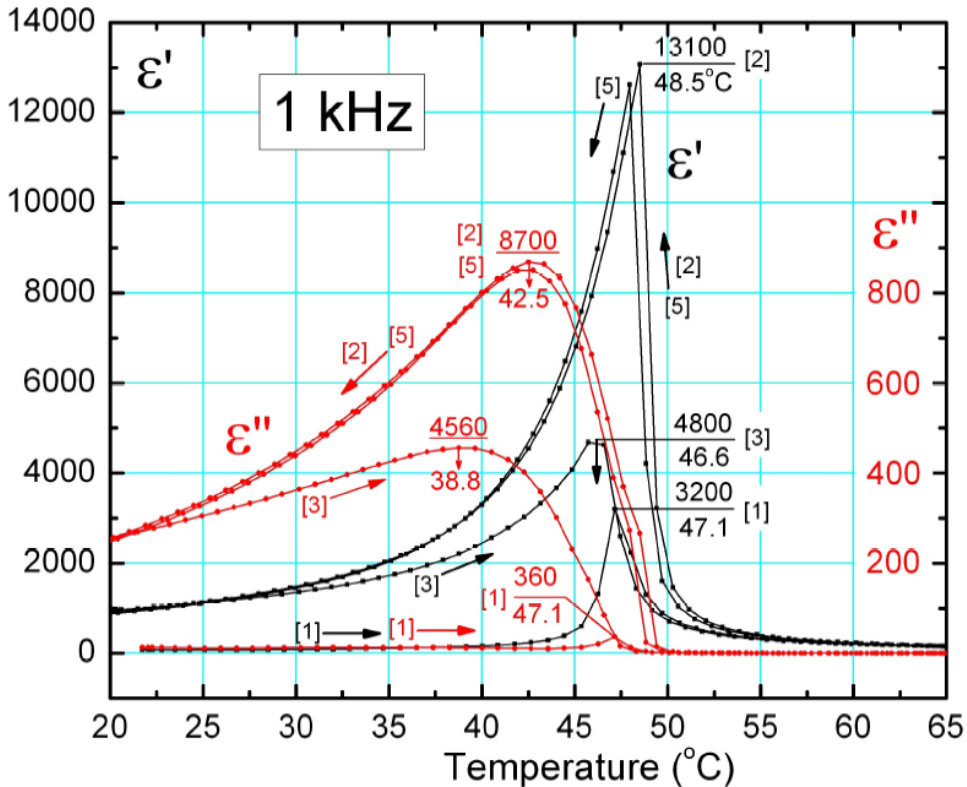


Fig. 2. The permittivity components variation during the 5 segments of temperature measurements. Some particular values of ϵ' , ϵ'' and tiers ratios, at selected temperatures, can be seen in Table 1.

3. Results

3.1. Permittivity relaxation at 1 kHz.

Temperature dependence of both components of permittivity was drawn for several frequencies during the

stages 1, 2, 3 and 5. A typical example is presented in Fig.2, at the frequency of 1 kHz. The imaginary component ϵ'' (the right hand side ordinate) is about one order of magnitude smaller than ϵ' .

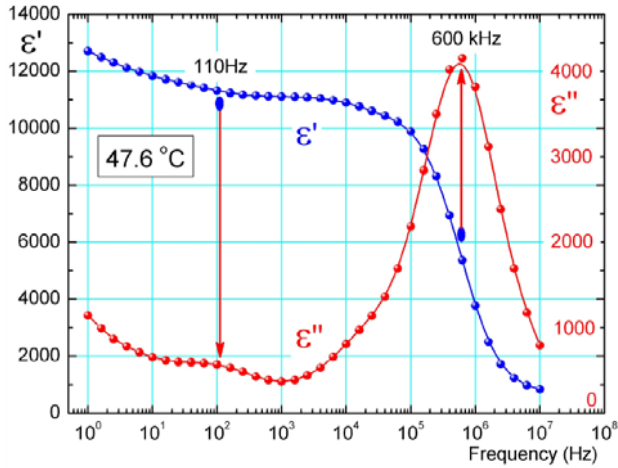


Fig. 3. The frequency dependence of the real and imaginary components of permittivity in the stage {2} in the ferro phase near the Curie point. The peak values of ϵ'' are correlated with the stepwise decrease of ϵ' .

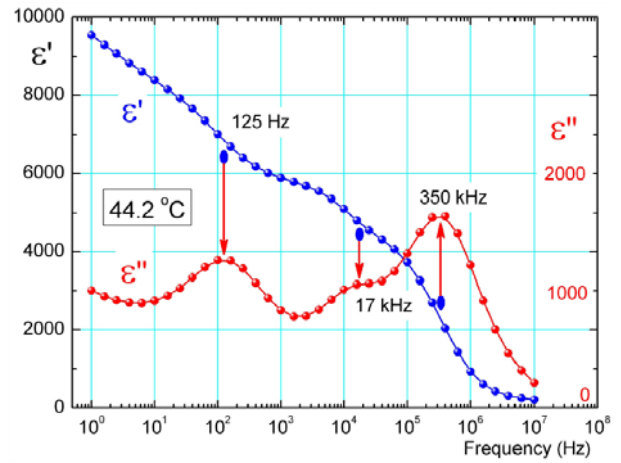


Fig. 4. Important changes in frequency dependence of permittivity components take place near the turning point 45°C (see figs 9 and 10). A middle relaxation component appears around 45°C (see Figs.5 and 6).

Table 1. Permittivity values in several stages at selected temperatures.

Temperature ($^{\circ}\text{C}$)	ϵ'				ϵ''			
	{1}	{2}	{3}	Ratio {2}/{1}	{1}	{2}	{3}	Ratio {2}/{1}
25	72	1120	1100	16	112	3340	3050	30
30	88	1450	1360	17	120	4440	3620	37
35	112	2050	1720	18	128	6000	4240	47
40	166	3300	2440	20	120	7970	4500	66
45	510	~7000	4200	14	125	~7400	2200	59

The stages {2} and {5} follow almost the same route for both components, as previously mentioned. The real component ϵ' , has more than one order of magnitude higher values on the stage {2} versus stage {1}, between 25 and 45°C (see Table 1). Particularly, component ϵ'' has increased 30 to more than 60 times versus stage {1}. These figures suggest important changes of domain configuration during relaxation. On the stage {3}, both components have smaller values versus stage {2}. There is a continuous relaxation, which according to our previous experiments extends on a very long time scale (see Figs. 4 and 5 in ref. [24]). According to present data, relaxation is much more slowly at temperatures lower than zero Celsius.

We also notice that the maximum values of ϵ'' , the imaginary component, in the stages {2} and {3} are displaced towards smaller temperatures and their position depends on the frequency (data not presented here).

3.2. Model of frequency dependence of permittivity components

The frequency dependence of both permittivity components at 47.6°C and 44.2°C , in the ferroelectric phase - stage 2, is presented in fig.3 and in fig.4. There are definitely two maxima of the component ϵ'' around 110Hz / 600kHz and 125Hz / 350kHz respectively, at lower and higher frequencies. There are two clear visible steps of ϵ' , the real component, associated with these maxima, which correspond to the relaxation times of the order $\tau_L \sim 10^{-3}$ sec and $\tau_H \sim 3 \cdot 10^{-7}$ sec.

At previously selected temperatures, as seen in fig.2 at 1 kHz, ϵ' decreases and ϵ'' increases with the temperature decrease. However, important changes take place on the entire frequency spectrum (see figs 3 and 4), particularly in the temperature interval T_{Curie} and $44/45^{\circ}\text{C}$. The ϵ'' , higher frequency maxima decreases, while the lower frequency maxima increases. This tendency is also clearly seen in Figs 5 and 6.

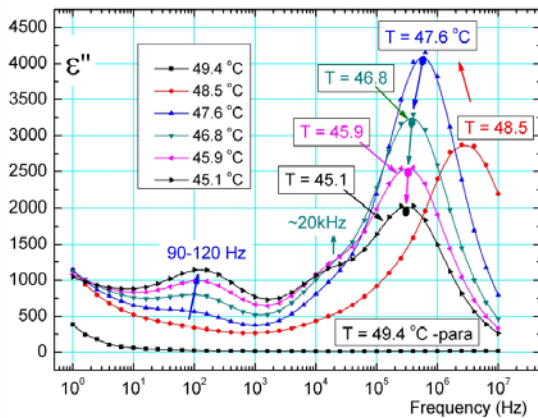


Fig. 5. Temperature evolution of the frequency dependence of ϵ'' component between the transition point (approximately 48.5°C) and the turning point 45°C . The decrease of higher frequency relaxation is correlated with the steeper increase of τ_H in Fig. 9, in the same temperature region.

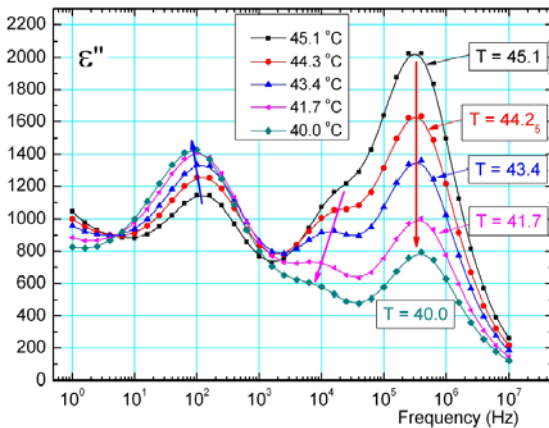


Fig. 6. Temperature dependence of peak evolution of the three relaxation frequencies. Between 45°C and 40°C the intermediate relaxation component (ϵ''_M) goes towards the lower frequency relaxation maxima of (ϵ''_L). However, its peak frequency value could not be precisely estimated in this paper.

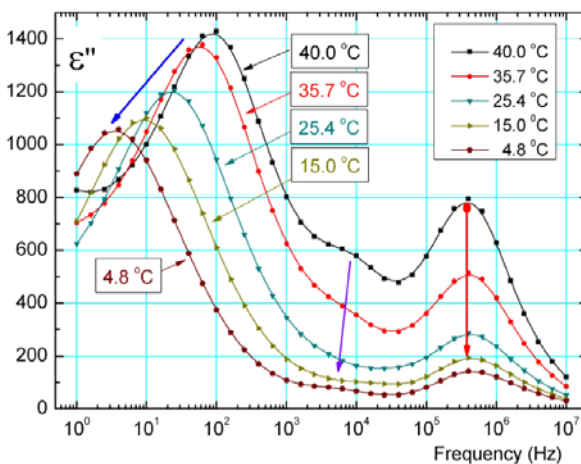


Fig. 7. In the temperature range 40°C - zero Celsius, the lower frequency component (ϵ''_L) substantially decreases and slides towards the lower frequencies. This is correlated with the Figs 8 and 10.

In Fig 4, at 44.2°C , a third maxima of ϵ'' appears around 17 kHz, as a shoulder near the 350 kHz maxima. The ϵ'' peaks temperature dependence are very important in understanding the nature of the relaxation mechanisms in the ferro phase of TGS crystal.

3.3. Temperature and frequency dependence of permittivity components.

There is a specific temperature dependence of permittivity components, on the entirely frequency spectrum 1 Hz - 10 MHz. Typical temperature and frequency dependence of the imaginary component are presented in fig. 5, 6 and 7.

The peak value and the high frequency relaxation of ϵ''_H decreases (τ_H increases), near the ferroelectric transition, i.e. on the interval $T_{\text{Curie}} \Rightarrow 45^\circ\text{C}$, in fig. 5. At the same time, the peak value and the low frequency relaxation of ϵ''_L increases (τ_L decreases), on the same temperature interval. Both dependences of the relaxation times τ_H and τ_L have been determined versus temperature, between zero and Curie temperature in fig 8.

In Fig. 6, the peak of the high frequency relaxation (ϵ''_H) continues to decrease, but keeps almost the same frequency relaxation, while the lower frequency relaxation continues to increase.

The intermediate relaxation component (ϵ''_M) has appeared in fig.6, as a shoulder near the high frequency maxima (ϵ''_H), around 45°C . It goes towards the lower frequency relaxation maxima (ϵ''_L) until about 40°C , in fig.7 and then apparently fade away at lower temperatures. There is no relevant data in the literature about this intermediate relaxation.

In Fig. 7, between 40°C and 15°C the low frequency relaxation maxima start to decrease and slides quite rapidly toward the lower frequencies. Around zero Celsius, the position of (ϵ''_L) maxima goes under 1 Hz and the frequency of the peak values could not be further estimated. However, the (ϵ''_H) maxima could be estimated at lower temperatures (see fig.9).

3.4. Relaxation time and the activation energy

Temperature evolution of the peak values of high and low frequency (ν) relaxation has been estimated from the graphics (like Fig 5, 6, 7). The relaxation time τ_H and τ_L have been calculated according to resonance classical condition $\tau_i \omega_i = 1$, that is:

$$\tau_i = 1/\omega_i = 1/2\pi\nu_i \quad (1)$$

Temperature dependence of both relaxation times is presented in log scale in fig. 8. Analytical dependences are also presented in Table 2.

Table 2. Temperature dependence of the relaxation time at high and low frequencies

	τ_H (sec)	τ_L (sec)
Fig. 8	$\log \tau_H = -7.1_1 + 0.0023_4 T$ (K)	$\log \tau_L = 9.6_3 - 0.039_5 T$ (K)
Fig. 9	NON-Arrhenius temp. dependence	$\tau_L(\text{sec}) = 1.02 \cdot 10^{-14} \exp [0.70 \text{ (eV)} / k_B T]$

The high relaxation time τ_H has weak non-Arrhenius temperature dependence. Details of temperature dependence can be seen in fig 8 and in fig.9. Between -40°C and $+40^\circ\text{C}$, τ_H has an insignificant variation of (3 to 4) 10^{-7} sec in fig.9. However, the very steep increase of τ_H between 48.5°C (approx. Curie point) and 45°C , of about one order of magnitude ($5 \cdot 10^{-7} \div 5 \cdot 10^{-6}$ sec), is quite unusual. The significant decrease of τ_H between 45°C and 40°C is also unexpected.

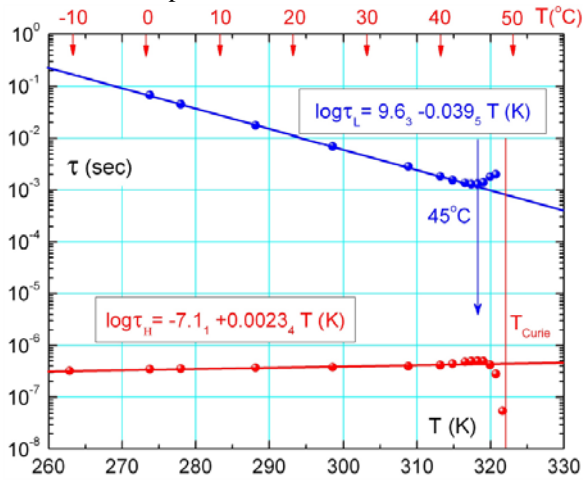


Fig. 8. Temperature dependence of τ_H and τ_L , the two relaxation times related with the main relaxation mechanism in TGS (see also Table 2).

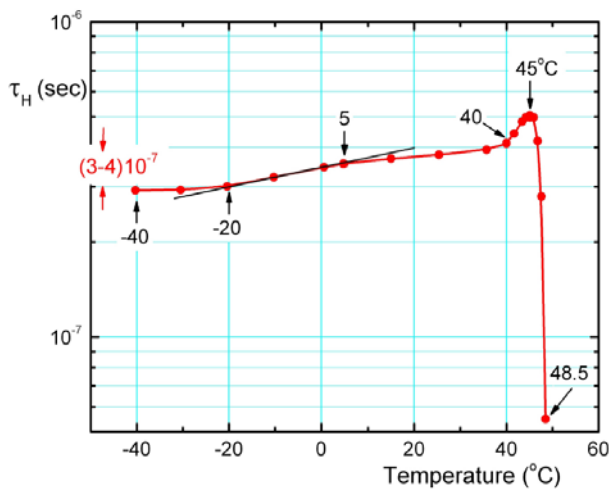


Fig. 9. The temperature dependence of τ_H , the relaxation time of higher frequency relaxation mechanism.

The temperature decrease of τ_L between zero and 45°C are presented in fig.8 and in fig.10. This dependence reveals a thermally activated mechanism of this relaxation. Data presented in fig. 10 give the following temperature dependence:

$$\tau_L = A \exp [\Delta E / k_B T] \quad (2)$$

here $A = 1.02 \cdot 10^{-14}$ sec. and the activation energy $\Delta E_L = 0.70 \text{ eV} \approx 28 k_B T$, (i.e. approx. 16 kcal/mol).

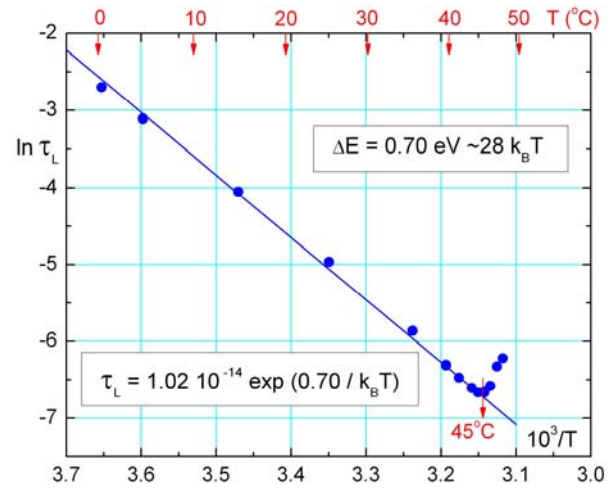


Fig. 10. The temperature dependence of τ_L , the lower frequency relaxation mechanism, suggests a temperature activated mechanism, in agreement with some literature data. See also Table 2.

Using another procedure (Cole-Cole representations [23]) for the TGS relaxation, Gilletta [25] has found $\Delta E_L = 0.70 \pm 0.02_5 \text{ eV}$. For several thickness of the samples he found the constant $A \approx (0.8 \div 7) 10^{-14}$ sec, close to our estimated value. A smaller activation energy of $0.42 \text{ eV} \approx 16 k_B T$ was equivalently estimated for the relaxation frequency $f_L = 1/2\pi\tau_L$ by Luther [10] in the ferroelectric region.

4. Discussions

Triglycine sulphate crystal (TGS for short), with the chemical formula $(\text{glycine})_3 \cdot \text{H}_2\text{SO}_4$ has two molecules in the unit cell [13]. Crystal has a monoclinic structure in the paraelectric phase and belongs to the centrosymmetric space group $P2_1/m$, having two mirror planes at $y=1/4$ and $y=3/4$ in the cell. In the ferroelectric phase, at

$T < T_C \approx 49$ °C, the mirror planes disappear and the space group becomes $P2_1$. The glycine group designed GI and SO_4^{2-} tetrahedra, are placed on the mirror planes [13]. The NH_3^+ group, pertaining to glycine GI, which is located asymmetrically versus the mirror planes, is the main responsible for polarization in the ferroelectric phase.

There are two distinct mechanisms involved in TGS relaxation.

The **higher frequency relaxation** mechanism (0.35 MHz, in fig.4), is called in the literature “the critical slowing down” mechanism [4, 5, 9-11]. A molecular relaxation mechanism, characteristic to ferroelectric transition (long distance order), seems to be related too. Apparently, it starts in the paraelectric phase, approaching the Curie point. The associated relaxation time, which is almost constant on a large temperature range in ferroelectric phase, $\tau_H = (3-4) \cdot 10^{-7}$ sec (see fig.9), suggests this mechanism is not influenced by the thermal energy, being rather related to higher energy lattice inter-cell interaction. A value of $\tau_H \sim 4 \cdot 10^{-7}$ sec was found by Zhang [5] in the temperature range above zero Celsius.

The **lower frequency relaxation** mechanism (110-125 Hz, in fig. 3 and fig. 4) is correlated to the dynamic of ferroelectric domains, having roughly a relaxation time $\tau_L \sim 3 \cdot 10^{-3}$ sec (fig. 8). An appropriate value of $\sim 2.3 \cdot 10^{-3}$ sec. was estimated in ref. [5], but no temperature dependence was given.

The relaxation time τ_L has an abnormal (non-Arrhenius) increase from ~ 45 °C to Curie point in fig.8 and in fig.10. The temperature dependence of the relaxation time τ_L suggests a thermally activated process in the temperature range down to 45 °C, due to the specific evolution of ferroelectric domains.

5. Conclusions

- Dielectric spectroscopy on the frequency range 1 Hz ÷ 10 MHz and on a large temperature range was used to study relaxation in the ferroelectric phase of pure TGS crystal, after crossing down the Curie point.
- The frequency dependence of the imaginary component of permittivity has been used, in a simple method, in order to study the relaxation process in TGS.
- Two fundamental relaxation mechanisms were identified in higher (MHz) and lower (~ 100 Hz) frequency range. The related relaxation time were in the range $\tau_L \sim 10^{-3}$ sec and $\tau_H \sim 10^{-7}$ seconds.
- The relaxation time $\tau_H = (3-4) \cdot 10^{-7}$ seconds is almost constant on $-40 / +45$ °C temperature range (figs.8 and 9). This relaxation related to “the critical slowing down” mechanism, reflect a long distance order in the lattice, which is not affected by the thermal energy (it has non-Arrhenius temperature dependence).
- The relaxation time τ_L shows Arrhenius temperature dependence, with an activation energy of 0.7 eV $\approx 28 k_B T$ on the temperature range $45 \rightarrow 0$ °C (fig.10 and table 2). It is related with the ferroelectric domains dynamics (relaxation).

References

- [1] S.B. Lang, D.K. Das-Gupta, *Ferroelectrics Rev.* **2**, 266 (2000).
- [2] Stephen Jesse, Arthur P. Baddorf, Sergei V. Kalinina, *Applied Physics Letters* **88**, 062908 (2006)
- [3] J. Fousek, V. Janousek, *Phys. Stat. Sol.* **13**, 195 (1966).
- [4] J. Zhang, *Ferroelectrics*, **281**, 105 (2002)
- [5] J. Zhang, *Phys. Stat. Sol. (a)* **193**, 347 (2002).
- [6] V. Tripadus, A. Radulescu, J. Pieper, A. Buchsteiner, A. Podlesnyak, S. Janssen, A. Serban, *Chemical Physics* **322**, 323 (2006).
- [7] Andrew P Giddy, Martin T Dove, Volker Heinei, *J. Phys.: Condens. Matter* **1**, 8327 (1989).
- [8] Genowefa Slosareki, A Heuerf, H Zimmermannf, U Haeberlent, *J. Phys.: Condens. Matter* **1**, 5931 (1989).
- [9] H.-G. Unruh, H.-J. Wahl, *Phys. Stat. Sol. (a)* **9**, 119 (1972).
- [10] G. Luther, *Phys. Stat. Sol. (a)* **20**, 227 (1973)
- [11] K. Kuramoto, H. Motegi, E. Nakamura, K. Kosaki, *J. Physical Society Japan*, **55**, 377 (1986).
- [12] S. Hoshino, T. Mitsui, F. Jona, R. Pepinsky, *Phys. Rev.* **107**, 323 (1957).
- [13] S. Hoshino, Y. Okaya, R. Pepinsky, *Phys. Rev.* **115**, 323 (1959).
- [14] H.V. Alexandru, C. Berbecaru, *Cryst. Res. Technol.* **30**, 307 (1995).
- [15] H.V. Alexandru, C. Berbecaru, *Ferroelectrics* **202**, 173 (1997).
- [16] H. V. Alexandru, C. Berbecaru, B. Logofatu, A. Stanculescu, F. Stanculescu, *J. Optoelectron. Adv. Mater.* **1**(4), 57 (1999).
- [17] H. V. Alexandru, C. Berbecaru, F. Stanculescu, L. Pintilie, I. Matei, M. Lisca, *Sensors and Actuators A* **113**, 387 (2004).
- [18] M. Costache, I. Matei, L. Pintilie, H.V. Alexandru, C. Berbecaru, *J. Optoelectron. Adv. Mater.* **3**, 75 (2001).
- [19] H.V. Alexandru, C. Berbecaru, *Mater. Sci. Semicond. Process.* **5**, 159 (2003).
- [20] H. V. Alexandru, *Annals New York Academy of Sciences* **1161**, 387 (2009).
- [21] E.T. Keve, K.L. Bye, P.W. Whipps, A.D. Anis, *Ferroelectrics* **3**, 39 (1971).
- [22] K.L. Bye, P.W. Whipps, E.T. Keve, *Ferroelectrics* **4**, 253 (1972).
- [23] K.S. Cole, R.H. Cole, *J. Chem. Phys.* **9**, 341 (1941).
- [24] H.V. Alexandru, C. Berbecaru, L. Ion et al, *Applied Surface Science* **253**, 358 (2006).
- [25] F. Gilletta, *Phys. Stat. Sol. (a)* **12**, 143 (1972).

*Corresponding author: horia@infim.ro